The Hénon–Heiles model

Daniel Larsson
University College of Southeast Norway

Abstract

In this report I will discuss the classical Hénon–Heiles model for the motion of a star around a galactic centre, first introduced in the (still very readable) paper [HH64]. I will also briefly mention why this model is important, historically, as well as in present day problems.

1 Introduction

Consider the motion of a star around a galactic centre. The motion has energy $H = K + V$, where K is the kinetic energy of the motion and V is the potential energy. Recall that in classical mechanics, K is dependent only on the speed of the star. We will study the possible trajectories the star traces out around the galactic centre in an idealized two-dimensional model. The model we will use is a classical model introduced by the two astronomers Michel Hénon and Carl Heiles in 1964 and can be considered the starting point of the modern study of dynamical systems and their complexity.

What Hénon–Heiles did was to introduce a potential function (and hence a force field) that they argued well approximated the force field a star is subject to in a galaxy (in particular the Milky Way). From this potential they constructed (via a standard technique in classical mechanics) a system of non-linear differential equations modelling the motion of the star. They then solved this system numerically with a computer (remember this was in 1964!) with a method called the four-step Runge–Kutta method, for different initial conditions. The results they found was very surprising and interesting. The model predicted a very complicated and erratic motion of the star for the energy in a certain range.

The results of Hénon and Heiles instigated a flurry of activity in non-linear dynamical systems and many more models[1] turned out to have complicated behaviour at certain parameter values of the model. Some of these models were known experimentally to have some peculiar quirks, but no theoretical study

[1] For instance, some chemical reactions, electrical circuits, biological systems, turbulent fluid flow, weather models, mechanical systems such as double pendulums and other types of oscillations, e.t.c., where shown to behave strangely under certain conditions.

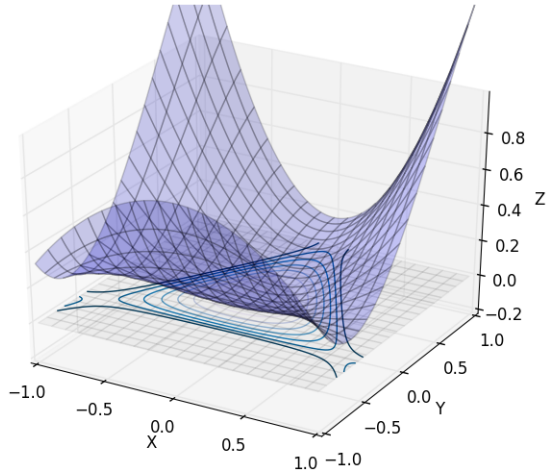

Figure 1: The Hénon–Heiles potential with contour curves

could show the true complexity of the systems until the Hénon–Heiles model appeared.

Nowadays, non-linear dynamical systems are essential for the study of important practical problems in almost all disciplines of science and engineering. For instance, models involving feedback and oscillations are almost always non-linear in real life. In this way, the Hénon–Heiles model, although not explicitly concerned with engineering[2], is a very important historical model, one that is simple to describe mathematically, but has very complicated behaviour, indicating the subtleties involved in studying real-life phenomena.

2 The Hénon–Heiles model

Instead of considering an actual star orbiting around a galactic centre, Hénon and Heiles considered a point mass (with normed mass = 1) orbiting around a central mass placed in origo in the (x, y)-plane. They decided to use the centrally symmetric conservative force field $\boldsymbol{F}(x, y) = \big(x + 2xy, y + x^2 - y^2\big)^T$, with potential

$$\Psi(x, y) = \frac{1}{2}\big(x^2 + y^2\big) + x^2 y - \frac{y^3}{3}, \tag{2.1}$$

[2]It turns out though, that the Hénon–Heiles potential can be used to describe other physical systems, such as ions in magnetic fields.

as the attracting force[3]. This means that the force the star is under the influence of at the point (x_0, y_0), is given by

$$\boldsymbol{F}(x_0, y_0) = \big(2x_0y_0 + x_0, y_0 + x_0^2 - y_0^2\big)^T.$$

As mentioned above the total energy of the system, comprises of the kinetic energy K, which is function only of x' and y', and the potential energy $V = \Psi$, which a priori is a function of the four variables x, y, x', y'. However, in the Hénon–Heiles model, Ψ is only dependent on x and y.

The motion of the star P is parametrised by $\boldsymbol{q}(t) = (x(t), y(t))$, with speed $\boldsymbol{p}(t) = (x'(t), y'(t))^T$ (since $m = 1$, the momentum $\boldsymbol{p}$ is equal to the speed $\boldsymbol{v}$). Therefore, the kinetic energy is given by

$$K(\boldsymbol{p}) = K(x', y') = \frac{\boldsymbol{p}(t)^2}{2} = \frac{x'(t)^2 + y'(t)^2}{2} = \frac{1}{2}\big(x'(t)^2 + y'(t)^2\big).$$

From this we see that the total energy is given by the expression

$$\begin{aligned} H(\boldsymbol{q}, \boldsymbol{p}) &= K(\boldsymbol{p}) + \Psi(\boldsymbol{q}) \\ &= \frac{1}{2}\big(x'(t)^2 + y'(t)^2\big) + \frac{1}{2}\big(x(t)^2 + y(t)^2\big) + x(t)^2y(t) - \frac{y(t)^3}{3}. \end{aligned} \tag{2.2}$$

Observe that the energy is implicitly dependent on time at this point.

What we will do now is to treat

$$(\boldsymbol{q}, \boldsymbol{p}) = (x, y, x', y')$$

as four independent variables, or as giving points in $\mathbb{R}^4$. Since these variables are functions of t, we see that as t varies we get a curve in $\mathbb{R}^4$. From now on we will also follow the classical convention and denote x' by p_x and y' by p_y. Notice that with this view-point, H becomes a scalar field of four variables.

2.1 The Hénon–Heiles potential

Let us look a bit at the potential $\Psi(x, y)$.

First of all we can note that close to the origin, the second-order term in $\Psi(x, y)$, $\frac{1}{2}(x^2 + y^2)$, will dominate over the other two (which are of order three), implying that around the origin the contour (and hence level) curves will be close to circular. This is clearly visible in Figure 2. This will give the potential an almost radial symmetry around the z-axis close to the origin.

We can also note that the other two terms will dominate when $x, y \to \pm\infty$ and $\Psi(x, y) \approx x^2y - \frac{1}{3}y^3 \to \pm\infty$ in the limits.

The regions in Figure 2 where the closed curves open up, i.e., in the direction of the y-axis and in the directions at angles $\pm 2\pi/3$ from this axis, are called the *exit basins*. The reason for this will become apparent in a while.

Suppose the star is at position (x_i, y_i) at time $t_i \geq 0$. Then the potential energy the star has at this point at the given time is $\Psi(x_i, y_i)$. Notice that

[3]They decided upon this specific choice by computer experimentation.

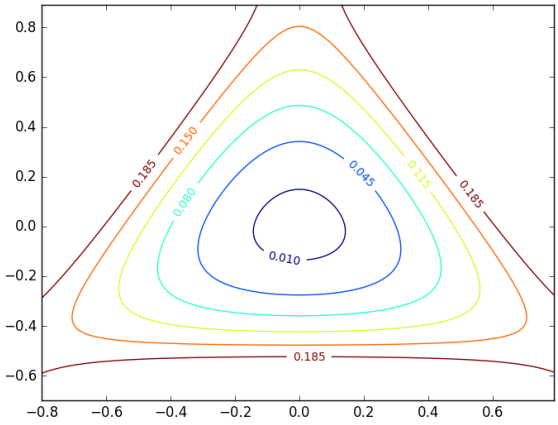

Figure 2: The contour curves of $\Psi(x, y)$.

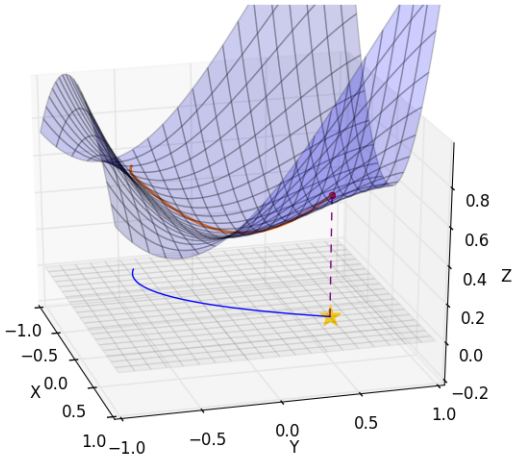

Figure 3: The star moving along trajectory with associated traced out potential.

the point $P_i = (x_i, y_i, \Psi(x_i, y_i))$ on the potential surface above (x_i, y_i) is a representation of this potential energy. Hence the motion of the star traces out a curve on the surface, lying directly above the trajectory of the star. See Figure 3.

2.2 The equations of motion

The physical system is governed by the Hamilton equations (which is more or less just a fancy version of Newton's second law)

$$\frac{d\boldsymbol{p}}{dt} = -\begin{pmatrix} \frac{\partial H}{\partial x} \\ \frac{\partial H}{\partial y} \end{pmatrix}, \qquad \frac{d\boldsymbol{q}}{dt} = \begin{pmatrix} \frac{\partial H}{\partial p_x} \\ \frac{\partial H}{\partial p_y} \end{pmatrix}. \tag{2.3}$$

With H given as in (2.2) one easily checks that the equations (2.3) become

$$\begin{cases} x' &= & p_x \\ p_x' &= & -x - 2xy \\ y' &= & p_y \\ p_y' &= & -y - x^2 + y^2. \end{cases} \tag{2.4}$$

Notice that this is a *non-linear* system of differential equations. We will see that this leads to very complicated and «unpredictable» motions of the star around the galactic centre. Notice that the system involves the vector field $\boldsymbol{F}$ as it should (in fact, $-\boldsymbol{F}$).

Important point. We will now order the variables as (x, p_x, y, p_y). Notice that this is consistent with the way the system (2.4) is written.

3 Simulations

We first discuss the set-up for the simulations.

Given initial conditions x_0, $p_{x,0}$, y_0 and $p_{y,0}$, a solution is four functions $x(t), y(t), p_x(t)$ and $p_y(t)$ in the variable t satisfying (2.4). Therefore these functions trace out a curve in $\mathbb{R}^4$ parametrized as

$$\boldsymbol{c}(t) = \big(x(t), p_x(t), y(t), p_y(t)\big).$$

Observe the order of the coordinates.

Since it is not so easy to visualize geometry in four dimensions we project this curve to $\mathbb{R}^3$ and $\mathbb{R}^2$:

$$\boldsymbol{c}(t) = \big(x(t), p_x(t), y(t), p_y(t)\big) \longrightarrow \boldsymbol{s}^{3d}(t) = \big(x(t), y(t), p_y(t)\big) \in \mathbb{R}^3 \tag{3.1a}$$

and

$$\boldsymbol{c}(t) = \big(x(t), p_x(t), y(t), p_y(t)\big) \longrightarrow \boldsymbol{s}^{\star}(t) = \big(x(t), y(t)\big) \in \mathbb{R}^2. \tag{3.1b}$$

We will also do another «projection» but we come to this shortly. Notice that the trajectory of the second curve is exactly the trajectory the star trace out around the galactic centre.

As with most non-linear systems, exact solutions to (2.4) do not exist. Therefore we are constrained to use numerical methods to solve it. We use the four-step version of Runge–Kutta for this purpose[4].

3.1 Fixing the energy

It turns out that it is reasonable to fix the energy. So suppose we fix the energy H to be E. This means we only look at the star trajectories that have energy E for all t. In particular, we have

$$\Psi(x,y) \leq E \quad \text{and} \quad \frac{1}{2}\big(p_x^2 + p_y^2\big) \leq E.$$

This implies that the trajectories of $\boldsymbol{s}^\star$, $\boldsymbol{s}^{3d}$ and $\boldsymbol{c}$ are all contained in a domain of finite measure[5], since if they were not, the star would simply disappear out of the galaxy (think about what happens if we allow $H \to \infty$).

From Figure 2 we see that somewhere between $\Psi(x,y) = 0.150$ and $\Psi(x,y) = 0.185$ the contour curves of the potential function goes from being closed to being open. The threshold energy turns out to be $1/6$. Below this value, the contour (and hence level) curves of $\Psi(x,y)$ are closed (and hence the energy is bounded) and above this the curves are open (and hence H is unbounded).

In fact, suppose $E \geq 1/6$ and that we chose initial conditions in the region where the contour curves of Ψ are closed (see Figure 2), then, eventually, the star will escape through one of the exit basins (hence the name) and will disappear to infinity (i.e., out of the galaxy); see Figure 11. If we were to chose initial conditions (with $E \geq 1/6$ still) in the regions outside where the contour curves are closed, the star will immediately disappear to infinity.

In conclusion, we let

$$0 \leq H \leq 1/6.$$

We will now treat H as a free parameter that we vary in this interval, and for fixed such $H = E$, we will study the motion of the star for different initial conditions.

One important consequence of fixing the energy is that we can reduce the number of variables. In fact, fixing $H = E$, we can re-write (2.2) as

$$p_x(t) = \pm\sqrt{2E - x(t)^2 - y(t)^2 - x(t)^2 y(t) + \frac{2}{3}y(t)^3 - p_y(t)^2}. \tag{3.2}$$

For simplicity, we consider only the positive square-root from now on. So this means that the only «real» variables (upon fixing $H = E$) is x, y and p_y.

[4]Consult virtually any textbook on differential equations for details on this method. I won't state the explicit algorithm here.

[5]By this I mean, area, volume and «four-dimensional volume» (which can be defined as the quadruple integral $\iiiint_{S\subset\mathbb{R}^4} dxdydudv$), respectively.

There is, however, one important point. to observe: we must still use p_x as a variable when we run Runge–Kutta. This is because the solutions to the system of equations is could be (at least in principle) sensitive to energy level. It could be that the solution that Runge–Kutta produces, at some point gives a p_x that is not compatible with (3.2) and the chosen energy level E (up to some chosen margin of error). This is something that has to be checked in every step of the numerical iteration and if at some point the difference between the p_x that Runge–Kutta produces and the p_x that (3.2) produces, lies outside this error interval, then we must disregard that trajectory and start over with new initial conditions[6].

When we have fixed our energy E, we must be careful when choosing initial conditions. We must take into account that

$$K(p_{x,0}, p_{y,0}) + \Psi(x_0, y_0) \leq E,$$

so this has to be checked when starting the simulation. In particular, since $\Psi(x_0, y_0) \leq E$, we must take initial positions inside the contour curve $\Psi(x, y) = E$.

3.2 Poincaré sections

The idea of a Poincaré section is to intersect the curve with a plane (or an arbitrary surface, for that matter). In our case, as we will intersect the (four-dimensional) curve, or rather trajectory, with the plane $x = 0$, it actually is the same as a projection (onto the yz-plane). However, we could equally well have chosen any other plane, but then the coding would be slightly more complicated, although the principle is exactly the same.

Figure 4 illustrates the idea. Suppose we have a trajectory, in $\mathbb{R}^3$ in the figure, and suppose we insert the plane $x = 0$. Then the *Poincaré section* of the trajectory, is the set of points the curve generates when it intersects the plane.

Notice that this defines an iterative map in the following way. Suppose the curve starts in a point p_0 in the plane $x = 0$. Then we integrate (i.e., calculate the trajectory) until we reach a point $p_1 = \pi(p_0)$ when the trajectory intersect the plane again. Integrating further we record the next time the trajectory intersects the plane, this time in the point

$$p_2 = \pi(p_1) = \pi(\pi(p_0)) = \pi^{(2)}(p_0).$$

Continuing in this manner we get a sequence of points $\{p_0, p_1, p_2, \dots, p_n, \dots\}$ in the yz-plane, with

$$p_{n+1} = \pi(p_n) \iff p_{n+1} = \pi^{(n)}(p_0).$$

The map π thus defined is the *return map* associated with the Poincaré section.

[6] I'm now uncertain that what I describe in this paragraph is actually necessary; it could be that this is automatic. The checks needed to make sure this condition is fulfilled might be one source of the tardiness of the computations.

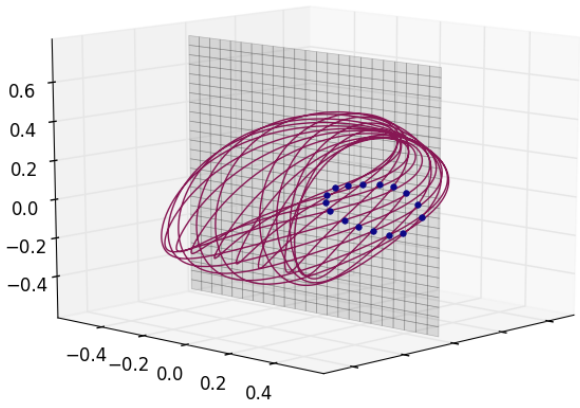

Figure 4: Poincaré section (blue dots) of the trajectory $x_0 = 0$, $y_0 = 0.4$, $p_{y,0} = 0.1$; $t_{\max} = 100$, $E = 0.100$.

One should, however, be aware that it is in general not possible to write down formulas for the return map in any sensible way.

What we will do, is not to plot the Poincaré section of each individual trajectory separately, but rather plot a whole range of sections for many trajectories (i.e., for many different initial conditions) of the same energy E in the same plot. In this way we can talk about the *Poincaré section of energy* E. We denote this ensemble by $\mathit{\Pi}_E$.

One point might deserve mentioning here. If we look at the section in Figure 4, we see that it appears that there are more instances of where the trajectory intersect the plane, than in the blue dots. This is a rather subtle point. Remember that the intersection actually occurs in four dimensions, not in three as we have depicted it here. In four dimensions the trajectory and the plane do *not* intersect in these points (only in the blue ones). This is one more instance of where our three-dimensional perception is failing us in applications to higher dimensions[7].

[7]The same phenomena appears already in lower dimensions. For instance, take the curve $\boldsymbol{c}(t) = (t, t^2 - t, t^2)$ in $\mathbb{R}^3$ and the straight line $y = x$ in $\mathbb{R}^2$. These two curves intersect only in the origin $(0, 0, 0)$. However, if we project $\boldsymbol{c}$ onto $\mathbb{R}^2$ we get another intersection point, namely $(2, 2)$ (the conscientious reader should check this!). So projection has produced an intersection that didn't really exist originally.

3.3 Computations

The computations were all done with code[8] written in Python 3 on a computer with an Intel 5, 2.6 GHz processor, and 8 GB ram. The computations of the Poincaré sections took a very long time to complete, indicating that the code could possibly be optimized, or better, have been written in C or C^{++}. It is somewhat unclear what kind of optimization in the present code could have produced a significant lowering of the computational time, making me lean towards the idea that Python might not be the best language for these types of heavy computations.

4 Results

4.1 The star trajectory $s^\star$

We start with the two-dimensional projection $\boldsymbol{s}^\star$ in (3.1b). As we mentioned before, the model is simplified so that the star only moves in the galactic plane, which we view as the xy-plane. The galaxy is centred with the origin in the (assumed) central (supermassive) black hole.

It is clear that the trajectory is dependent on the initial conditions: position (and hence potential energy) and momentum (and hence kinetic energy). By giving the initial conditions we therefore fix the start position (x_0, y_0) and start momentum $\boldsymbol{p}_0 = m\boldsymbol{v}_0 = (p_{x,0}, p_{y,0})^T$. From the theory of ordinary differential equations it follows that there is a *unique* trajectory (solution curve) $s^\star$ going through this starting point, and with the velocity as the tangent vector at this point. The integration of the motion (i.e., the numerical solution of the system of equations) then gives the whole star trajectory step-by-step (with the given step size) for as long as we would like.

It is however important to note that we use a numerical method for solving the system. Therefore there is a built-in error that has to be accounted for. The whole thing becomes even more complicated as the error can be magnified as the integration proceeds. This is nothing that will be of any concern for us now, but it is a very important and real issue that has to be handled rigorously in other practical applications.

We will later see another aspect of the model that is somewhat related to the error issue. Namely, so called *sensitive dependence on initial conditions*. This is not the same as the involvement of errors, which is built-in in the method of *solving* the system (or failure of accurately measure the initial conditions if we are looking at it from a practical point of view). Sensitive dependence on initial conditions is an inherent trait of the system or model.

[8] Which can be made available upon request.

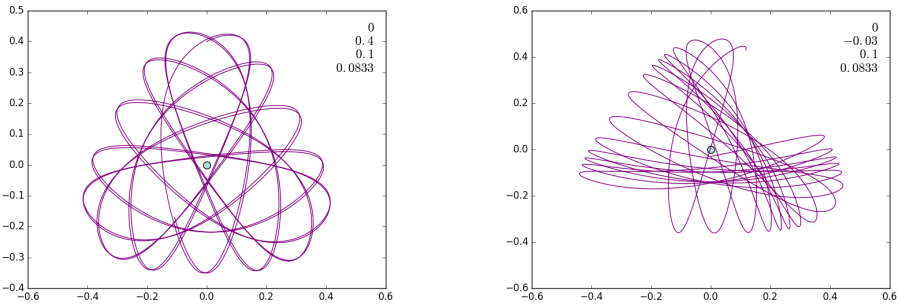

Figure 5: Two trajectories with energy $E = 0.833$, $t_{\max} = 100$.

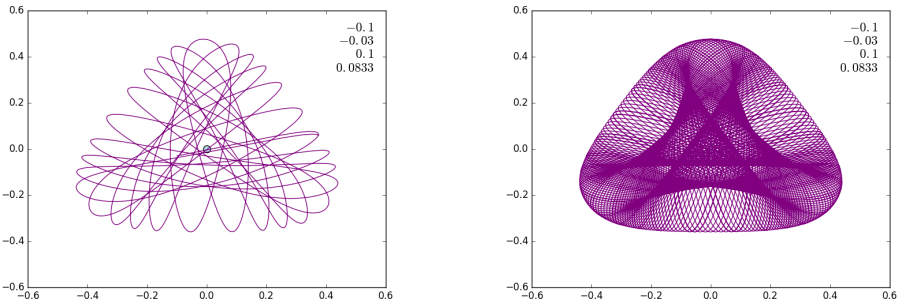

Figure 6: Same trajectory with $t_{\max} = 100$ and $t_{\max} = 1000$.

4.1.1 Plots

In the plots, Figures 12–10, the numbers in the upper-right corner indicates x_0, y_0, $p_{y,0}$ and E, respectively (from top to bottom). In Figure 11 is shown how, for energies higher than 1/6, the trajectories escape through (in this case two of) the exit basins.

4.1.2 Comments

There are three main points (which are connected) to notice with the plots:

(1) **Regular trajectories**. The first thing to notice is that all energies have some trajectories that are regular in the sense that they are more or less predictable and that there is a clear pattern involved. This does clearly not exclude the possibility that the trajectories can be quite complicated. One can also notice that, independent on the complexities of the trajectories, they always occupy a bounded region (of finite area) in the plane.

(2) **Sensitive Dependence on Initial Conditions** (SDIC) at higher en-

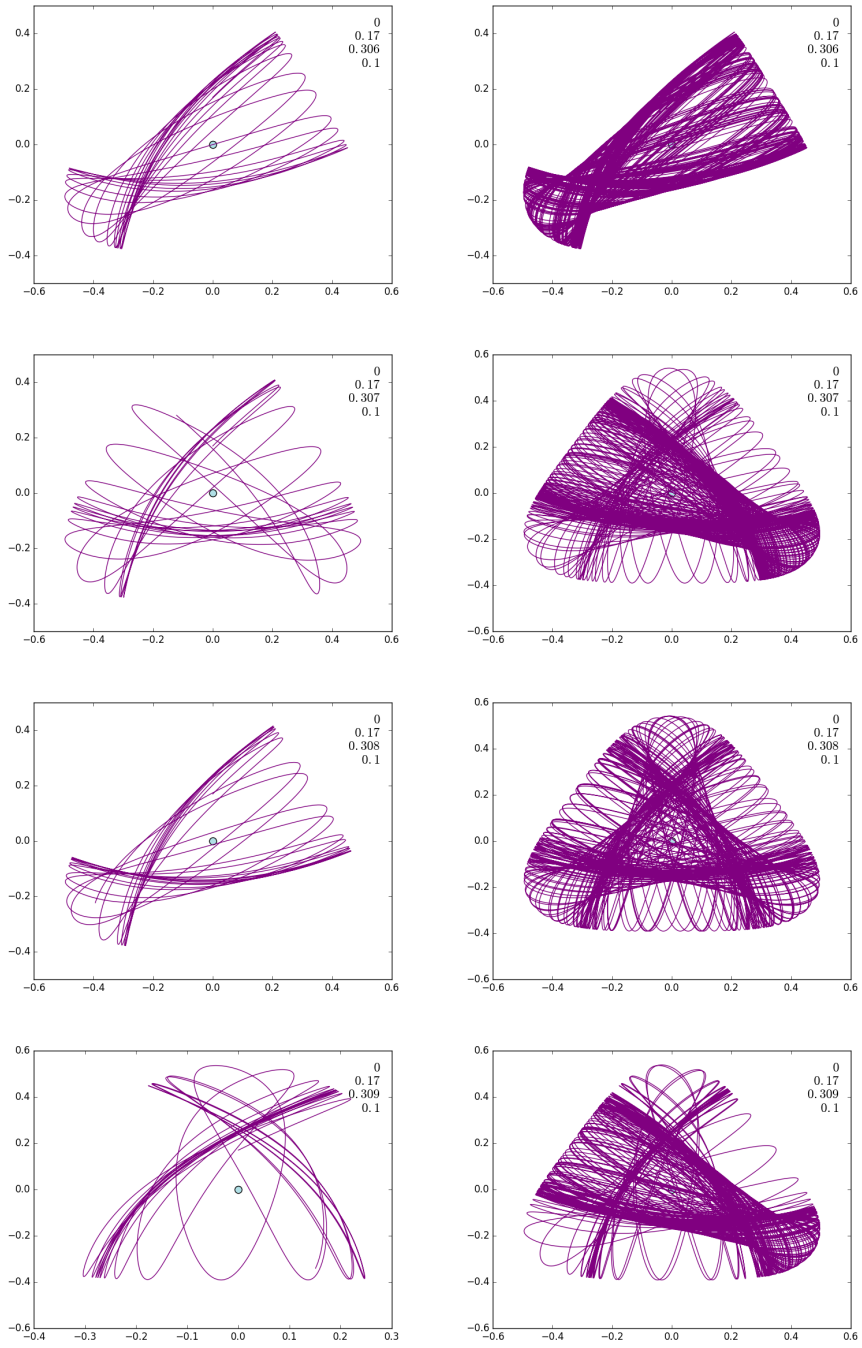

Figure 7: Observe that a slight change in one initial condition give big change in trajectory; $t_{\max} = 100$ and $t_{\max} = 1000$, $E = 0.100$.

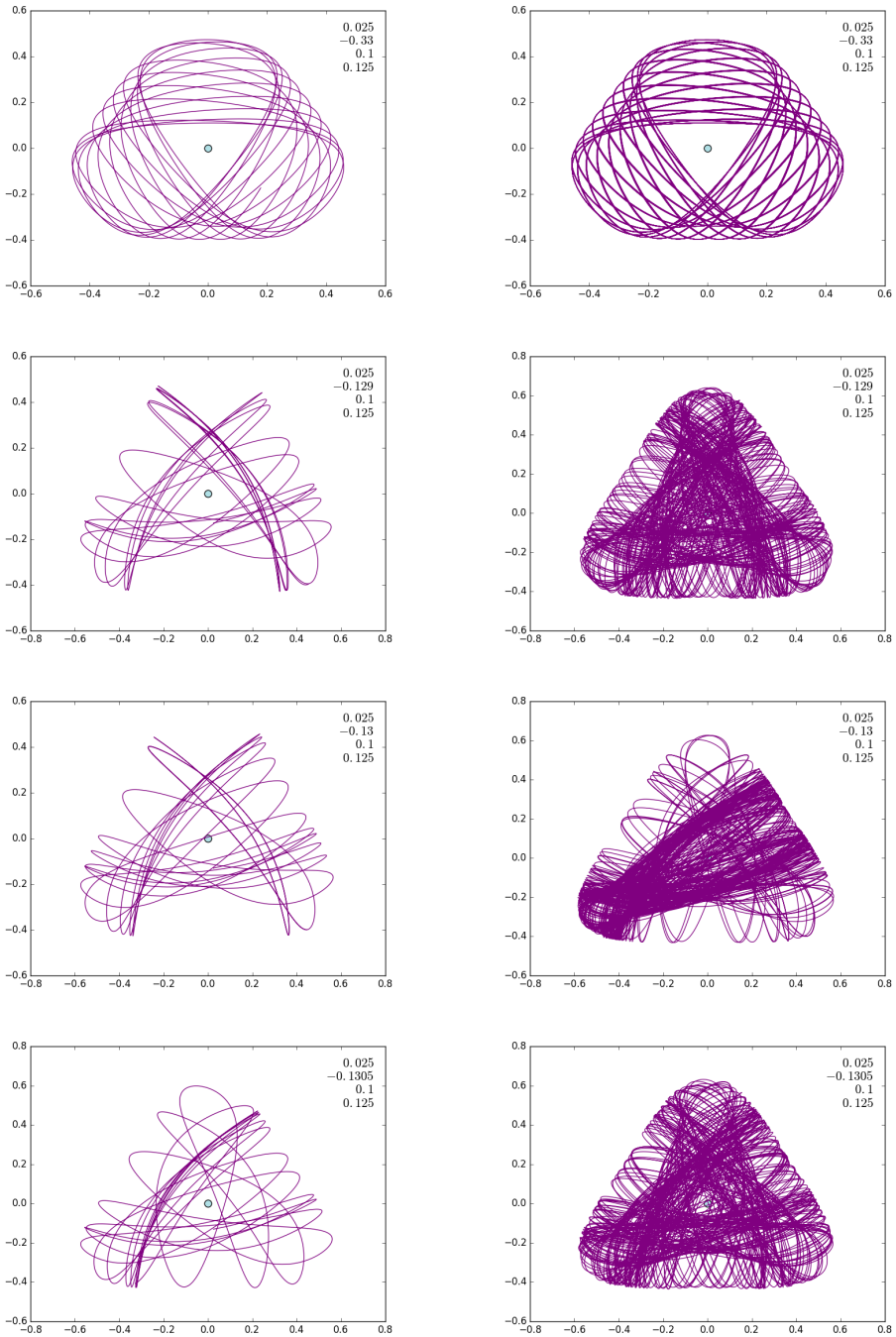

Figure 8: Observe once again the slight change in one initial condition giving a big change in trajectory; $t_{\max} = 100$ and $t_{\max} = 1000$, $E = 0.125$.

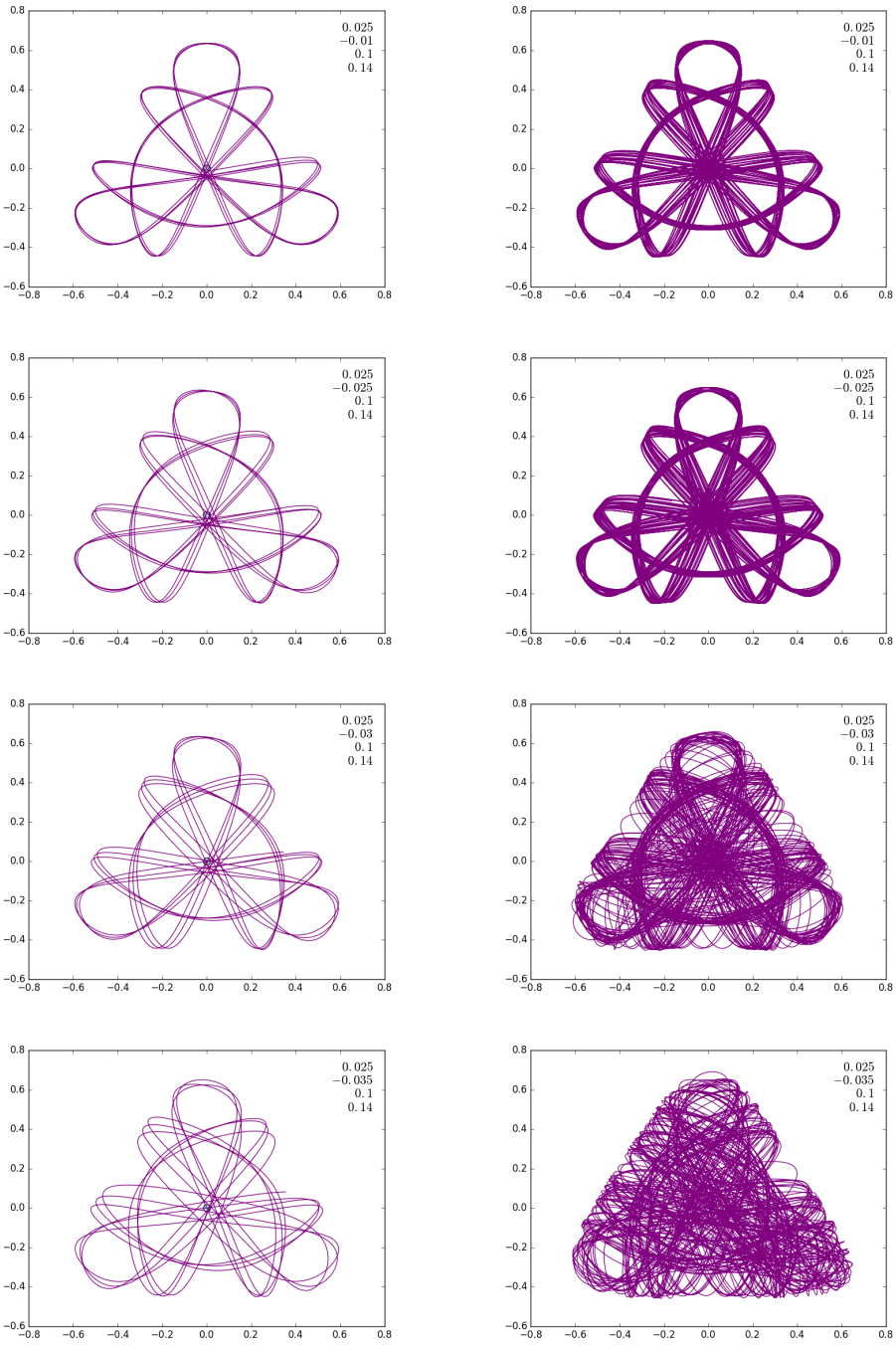

Figure 9: Observe once again the slight change in one initial condition giving a big change in trajectory; $t_{\max} = 100$ and $t_{\max} = 1000$, $E = 0.140$.

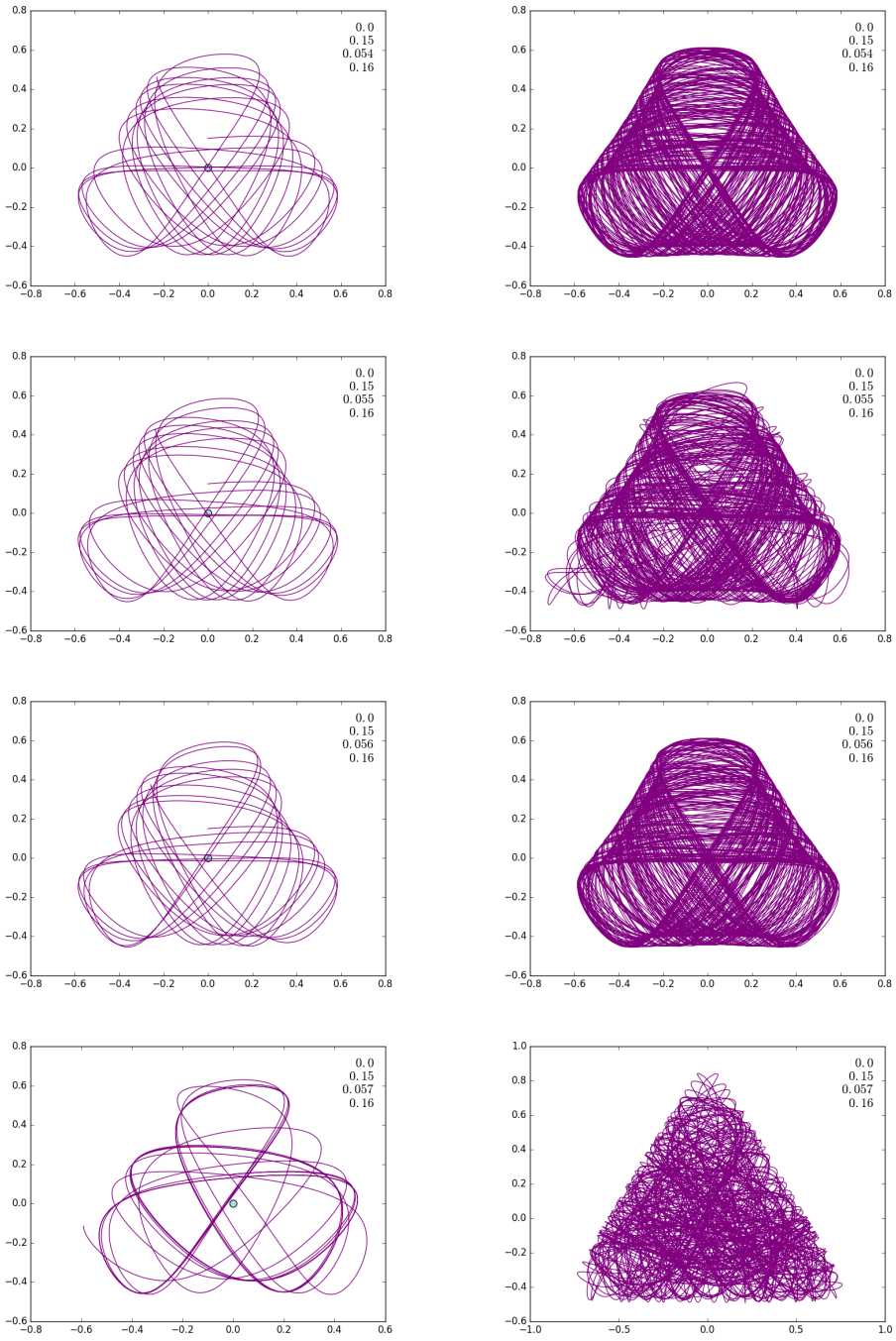

Figure 10: Observe once again the slight change in one initial condition giving a big change in trajectory; $t_{\max} = 100$ and $t_{\max} = 1000$, $E = 0.160$.

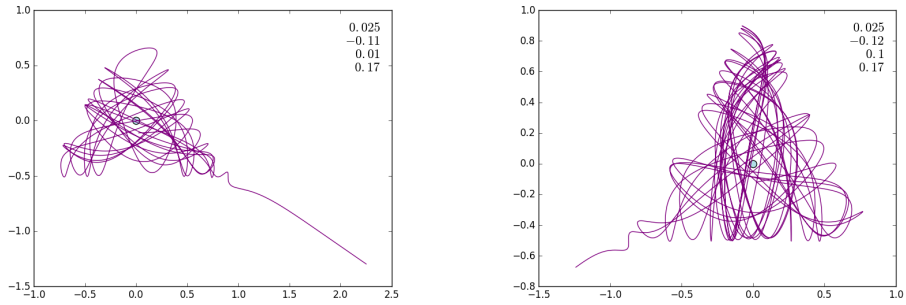

Figure 11: Trajectories escaping through two of the exit basins.

ergies. The next thing to observe is that, as the energy increases, the sensitivity of the geometry of the trajectories are very sensitive to changes in initial conditions. In other words, changing the initial conditions ever so slightly can change the long-term behaviour of the motion significantly. See for instance Figure 7 and the figures following that. This observation leads to the next one:

(3) **Chaotic trajectories**. When the energy increases above a certain threshold (which is about $E = 1/12$) the long-term behaviour can be very complicated and lack any kind of clear pattern or structure. Such trajectories are called *chaotic*. There is a very close connection between sensitive dependence on initial conditions and chaotic trajectories: chaotic trajectories tend to be very sensitive to changes in initial conditions, and vice versa. For instance, when $E = 0.160$, one can note that there is a transition from a disordered trajectory to a more ordered one, and then to disorder again, as $p_{y,0}$ increases from 0.055 to 0.057, via 0.056.

However, that a trajectory is chaotic does not mean that there are no *global* symmetries involved. This can be seen for instance in Figure 7 where (in the cases $x_0 = 0.025$, $y_0 = -0.125$, $p_{y,0} = 0.1$ and $y_0 = -0.13$) there are global symmetries, but locally (around the origin for instance) there are no discernible patterns.

One can also notice that the short-term behaviour can be quite regular, but as time goes on, this behaviour then transitions into a quite disordered behaviour. As an example of this see the last two initial conditions in Figure 10.

The above snap-shots does not quite convey the true complexities involved. In fact, the higher the energy the more chaotic the trajectories become. When $E = 0.160$, essentially all initial conditions will lead to chaotic behaviour of the trajectory in the long term. This will become apparent when we look at the Poincaré sections Π_E below.

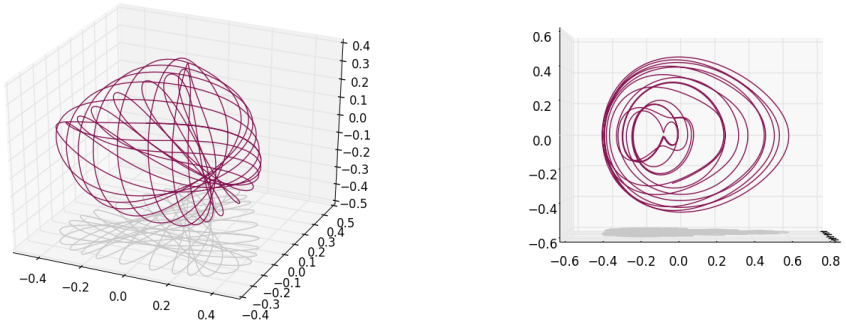

Figure 12: The same trajectory viewed from different angles; $E = 0.833$, $t_{\max} = 100$.

One last thing to notice with the plots is that the global geometric form bounding a trajectory seems to be quite familiar. Namely, a trajectory of constant energy E lies wholly inside the contour curve of potential energy $\Psi(x, y) = E$. This is naturally not a coincidence and can be explained from the inequalities bounding the initial conditions as in section 3.1). When the trajectory is chaotic, we see that it tends to fill out the whole domain inside the contour curve. This is actually an indicator of chaotic trajectories.

4.2 The three-dimensional projection s^{3d}

We will now look at the three-dimensional plots with coordinates ordered as (x, y, p_y). In the plots, the trajectory is projected onto the xy-plane showing that this does indeed give the trajectory as in the previous plots. So, a point (a, b, c) on this three-dimensional trajectory represents the position (a, b) of the star and the y-coordinate of the momentum c at that point (a, b).

For each trajectory, we present two views, one giving the placement of the trajectory in $\mathbb{R}^3$ and one indicating the projection on the yp_y-plane. Hence these two plots are simply the same trajectory, but viewed at different angles. The un-numbered axis is the x-axis.

4.2.1 Plots

See Figures 13–16.

4.2.2 Comments

Notice that even when the energy goes up, there are trajectories with regular behaviour (which we already remarked upon). This is quite clear from the view

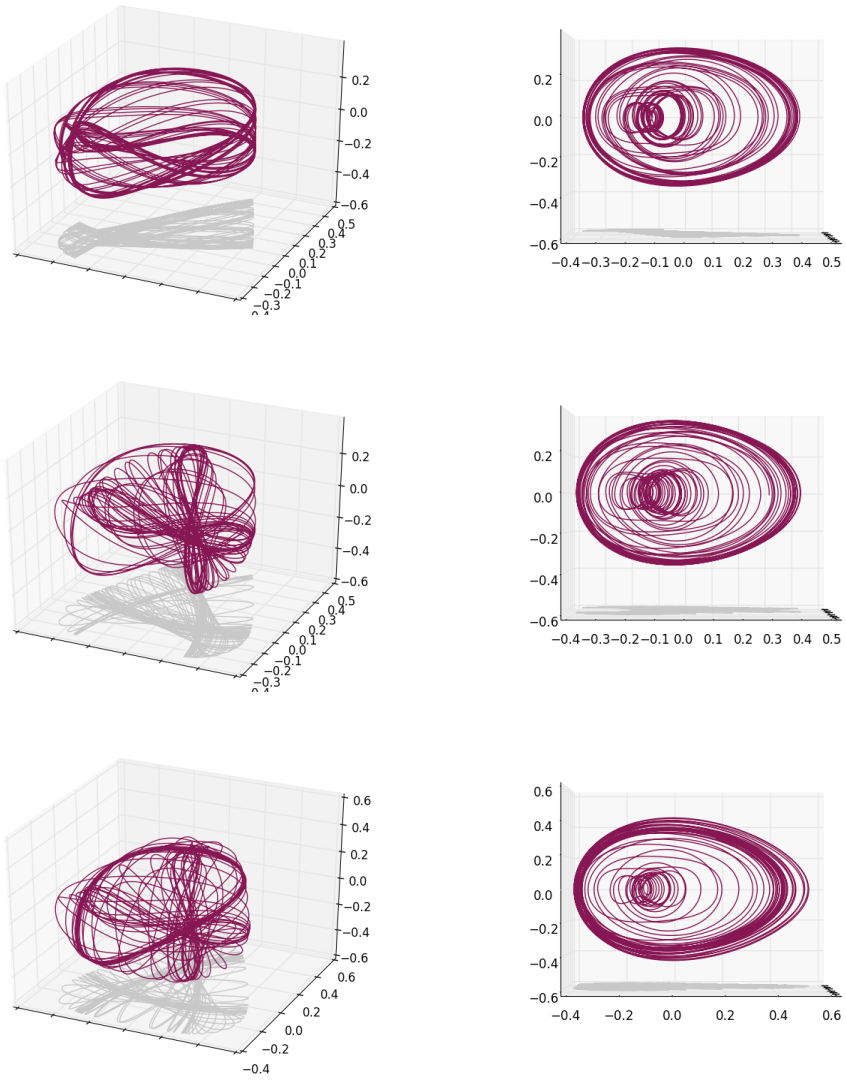

Figure 13: Observe that a slight change in one initial condition give big change in trajectory; $t_{\max} = 300$, $E = 0.100$.

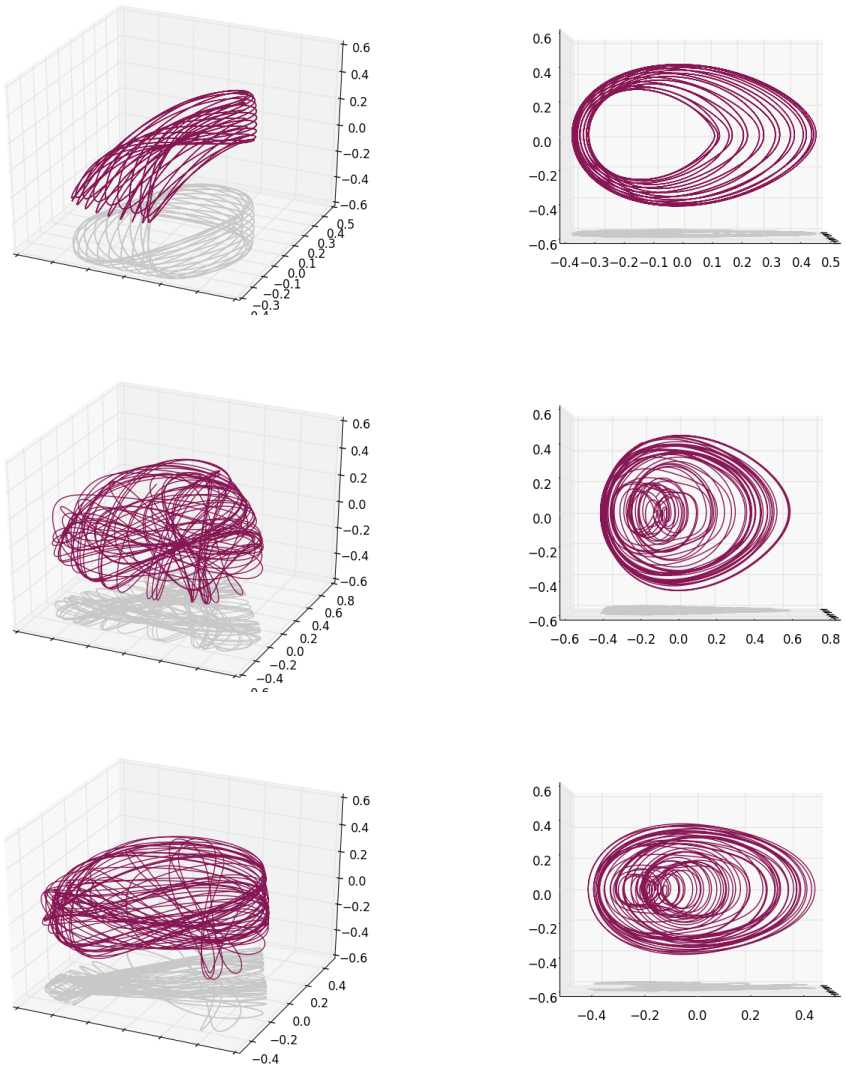

Figure 14: Observe that a slight change in one initial condition give big change in trajectory; $t_{\max} = 300$, $E = 0.125$.

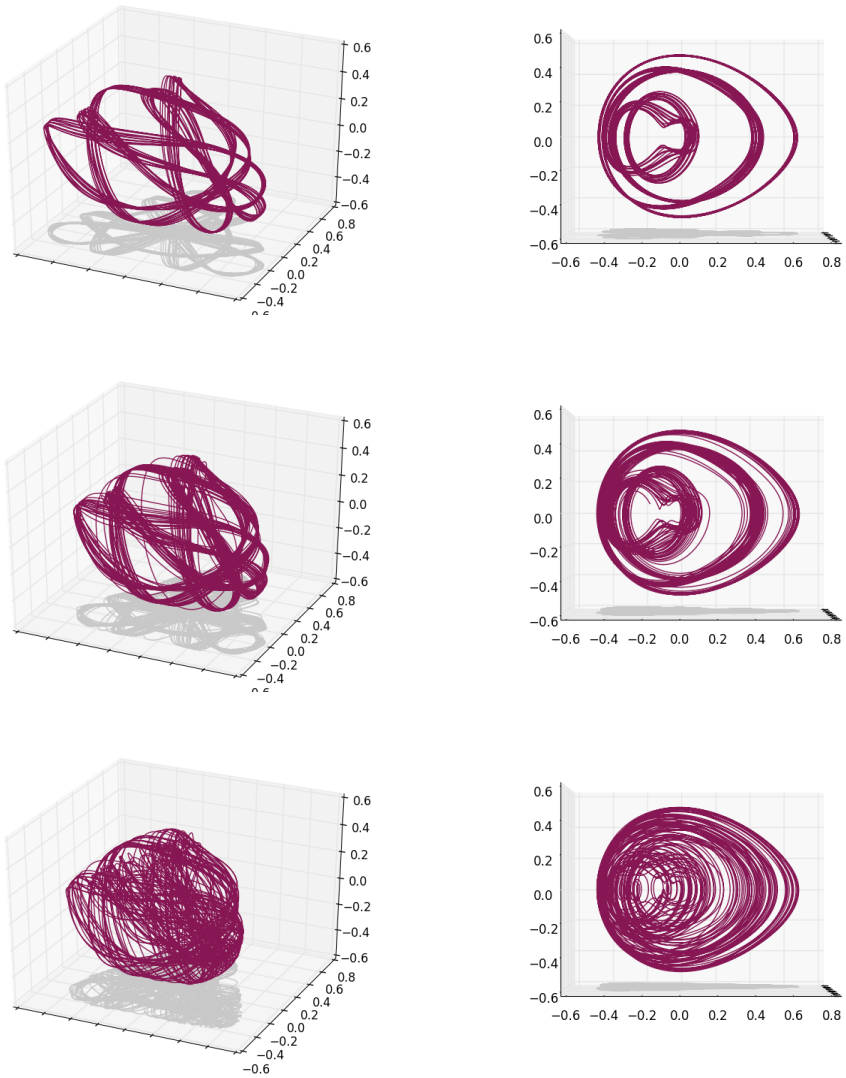

Figure 15: Observe that a slight change in one initial condition give big change in trajectory; $t_{\max} = 300$, $E = 0.140$.

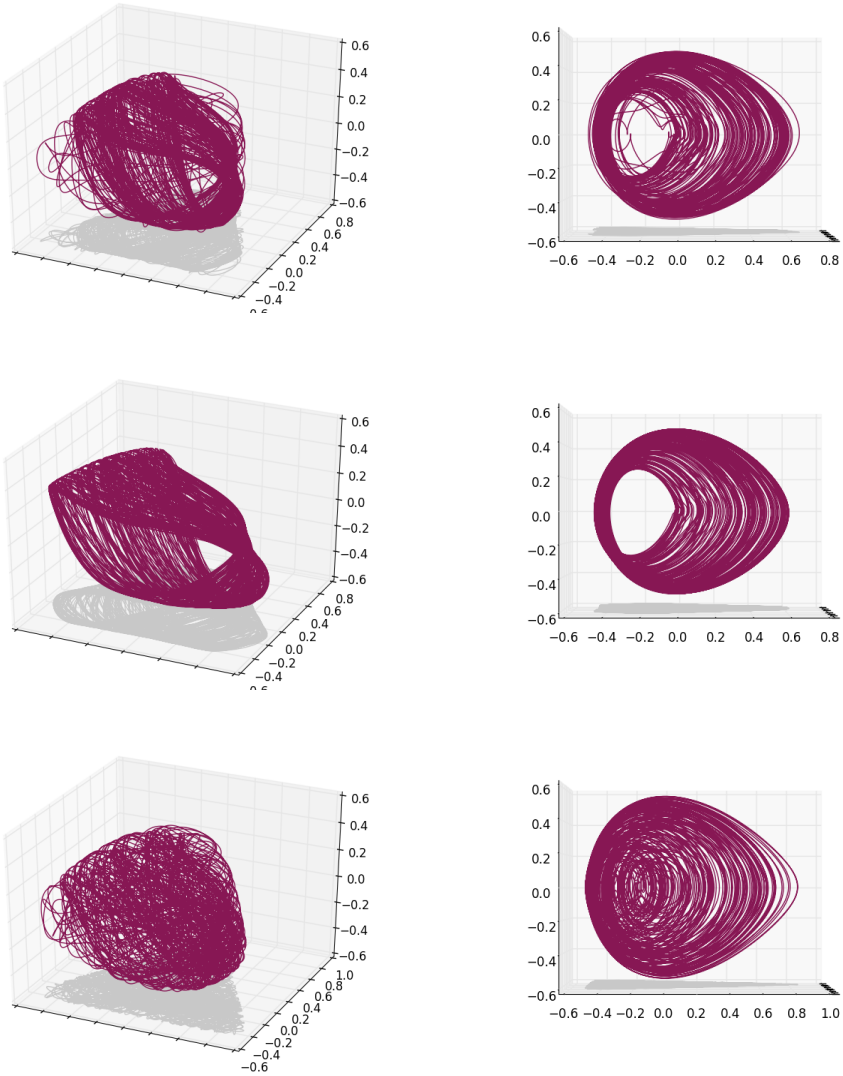

Figure 16: Observe that a slight change in one initial condition give big change in trajectory; $t_{\max} = 1000$, $E = 0.160$.

of the yp_y-plane. Notice also that the trajectories are bounded in volume (we can embed the trajectories in a sphere of radius at most one, for instance).

4.3 The Poincaré sections Π_E

We now turn to the Poincaré sections Π_E and these show the true complexity of the model (in the energy spectrum $0 \leq E \leq 1/6$ that we are interested in). As we mentioned before, the essential feature of these Poincaré sections is that it takes into account *all* the initial conditions at the same time. Starting with an initial condition $(x_0, p_{x,0}, y_0, p_{y,0})$ we integrate successively to get the trajectory in $\mathbb{R}^4$ and record all the points where the trajectory intersects the plane $x = 0$. Then we move on to the next initial condition and repeat the procedure. We do this for all initial conditions that are permissible for the fixed energy E.

4.3.1 Plots

In Figure 17, we first look at the Poincaré sections for one choice of initial condition and varying energies, before looking at the sections Π_E. Finally, in Figure 18 we present the full Poincaré sections for the energies $E = 0.03$, 0.055, 0.0833, 0.100, 0.125, 0.140 and 0.160.

4.3.2 Comments

The primary comment to be made is that, clearly, the dynamics and behaviour of the star become very complicated for higher energies in the interval $0 \leq E \leq 1/6$. The trajectories hit the plane $x = 0$ in a completely unordered fashion. However, even in the highest energy case, there are small «islands of tranquillity» where the trajectories behave somewhat regularly.

Let us begin by looking at Figure 17. In the first section where $E = 0.1$, we see that the trajectory is very regular. It is not periodic, but *quasi-periodic*: the trajectory hits the plane along a well-defined closed curve. If it were periodic it would hit the plane $x = 0$ in the same point over and over, and hence the section would simply be a point.

Increasing the energy slightly to $E = 0.106$, we see that the curve seems to split up into small «sub-curves». In the regions where this occurs there are indications that the trajectory is slightly chaotic[9]. Increasing the energy further (notice that the increase is not significant), we see that the splitting has occurred and the trajectory hits the plane along several closed curves, in addition to some curves that appear to be non-closed[10]. Then increasing the energy ever so slightly once more we see that the trajectory turns into a chaotic one: it hits the plane in regions where there are no obvious pattern (this can actually be proven rigorously). But we still see that the trajectory (remember

[9] I'm not quite sure this is the case: it could simply be that I didn't run the simulation long enough to discern any pattern.

[10] This is probably not the case. If we were to zoom in on these non-closed curves we would in all likelihood see that they are, in fact, closed.

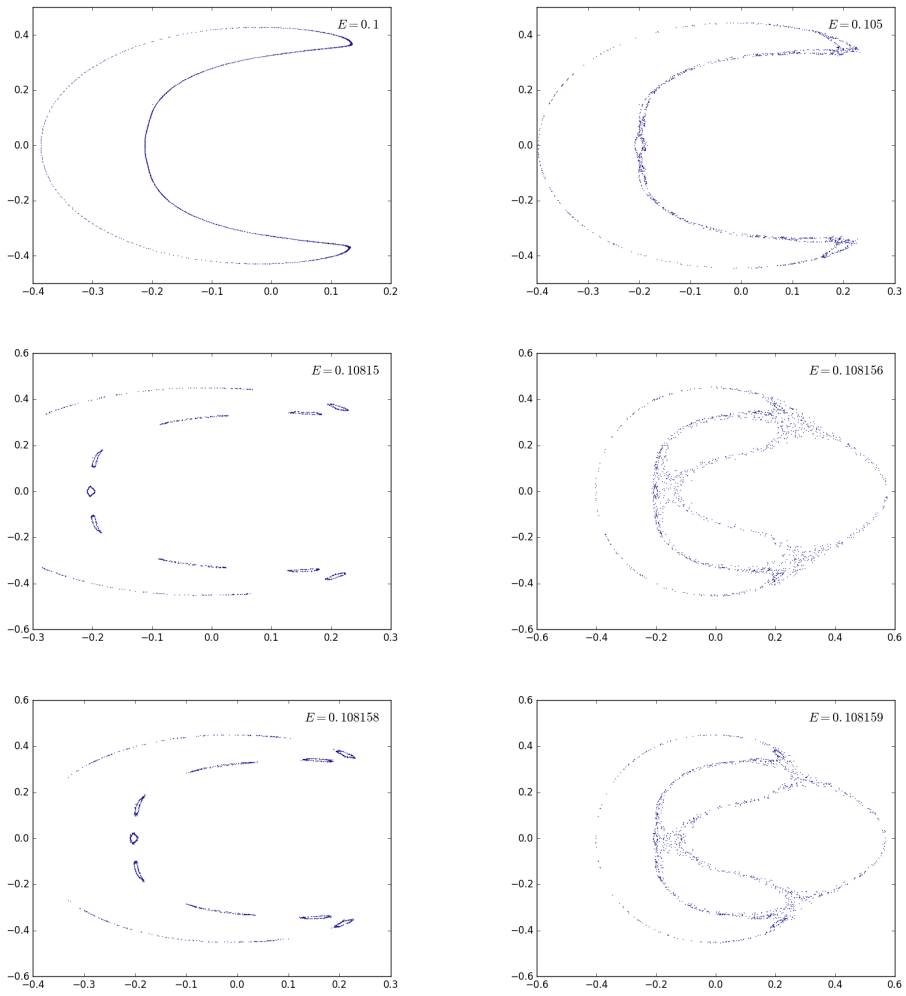

Figure 17: Poincaré sections of one trajectory with initial conditions $x_0 = -0.03$, $y_0 = -0.02$, $p_{y,0} = 0.15$. Observe that a slight change in energy can turn the trajectory into a chaotic one.

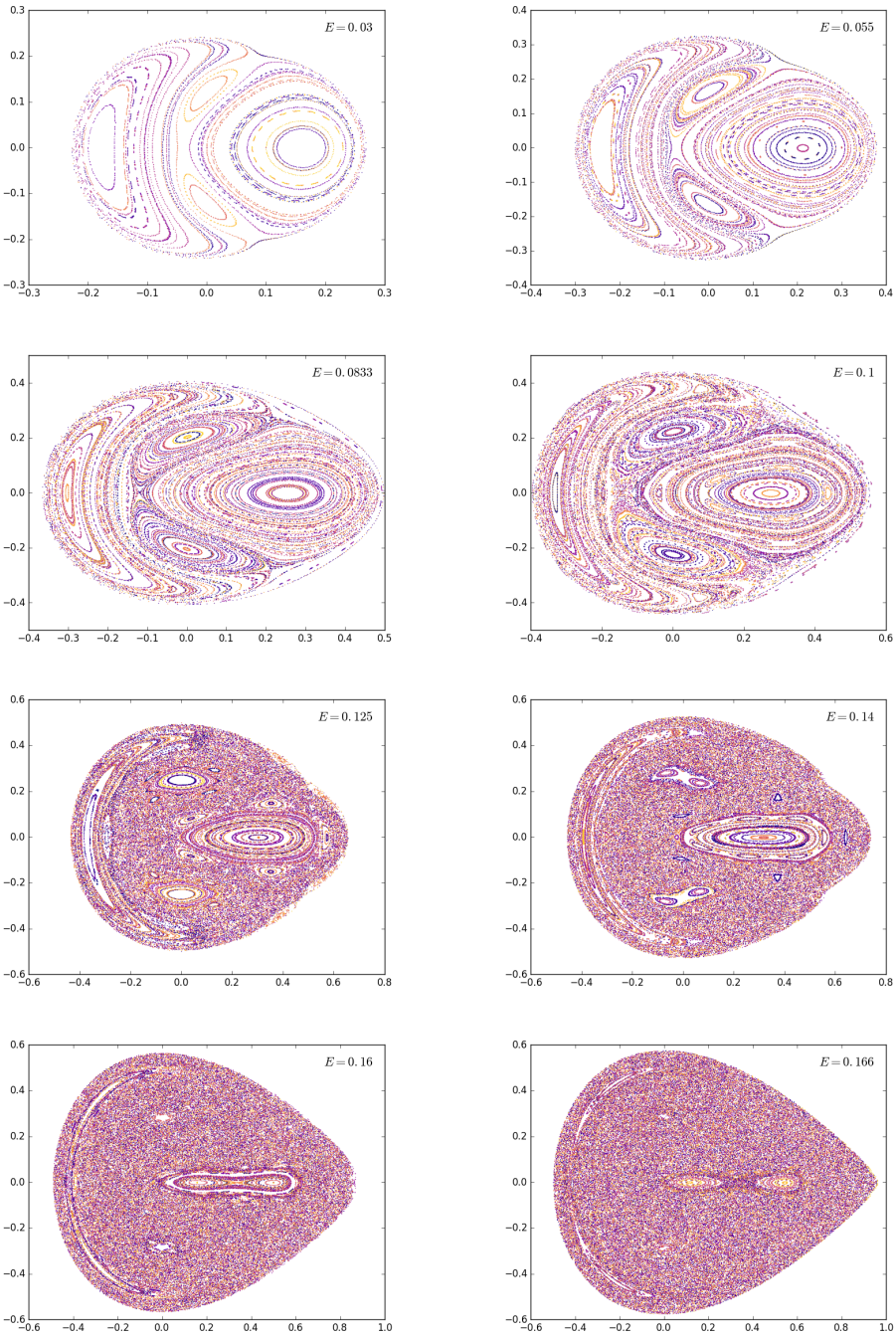

Figure 18: Poincaré sections of the Hénon–Heiles model for the indicated energies; $t_{\max} = 1000$.

that this is still only *one* trajectory describing the motion of the star) hits the plane in some regions where there are closed curves, indicating that the trajectory is a mix of being quasi-periodic and chaotic.

When increasing the energy infinitesimally again, we see that the trajectory goes from chaotic to ordered, and then, increasing further, it goes into a mix of quasi-periodicity and chaotic again. This is a clear example of SDIC.

Now, looking at the complete Poincaré sections Π_E in Figure 18, we see that for low energies, below $E = 0.0833$, there are only quasi-periodic solutions and a few periodic ones, which can be seen as small dots inside the closed curves. The different colours are meant to represent different trajectories[11].

Increasing the energy to $E = 0.0833$ we can see that the trajectories are still mostly quasi-periodic, but there are small regions where there are chaotic trajectories (or, rather, where trajectories hit the plane in a chaotic fashion). For energies higher still, we see clearly that the regions where the trajectories are chaotic dominates completely over the quasi-periodic ones, and finally, when $E = 0.160$, there are almost no quasi-periodicity left.

5 Conclusions

5.1 Model specific conclusions

In this report we have looked at the Hénon–Heiles model for a star moving in the planar potential field Ψ generated by a galactic centre. For energies in the region $0 \leq E \leq 1/6$ it turned out that the trajectories that the star follows can be very complicated. In particular, it turned out that a slight change in initial conditions for the star can produce a significant change in the trajectory, for instance, going from an ordered (quasi-periodic) solution to a completely disordered (chaotic) solution.

The manner in which we studied this model was that, starting from the potential $\Psi(x, y)$, we constructed, via some black(-box) magic, a system of *non-linear* ordinary differential equations, describing the motion of the star. This system was solved numerically for fixed energy with the four-step Runge–Kutta method. We did this for different initial conditions and the solutions was represented in three different ways:

(i) the actual planar trajectory the star traces out;

(ii) the three-dimensional trajectory with the z-axis representing the y-coordinate of the star's momentum, and finally,

(iii) the Poincaré sections, where we bundle «all» initial conditions together in one plot, giving a two-dimensional projections of a four-dimensional curve.

This was all done for different energies and compared.

[11] One should be aware, however, that since there are more trajectories than colours (at my disposal) many trajectories share the same colour.

5.2 General conclusions

Although we have studied a specific model, with a specific potential function, the behaviour of this model is not an isolated pathology. In fact, this is a phenomena that is prevalent in many (if not all) «real life» systems where there is some non-linear part. For instance, oscillations (and vibrations) with periodic damping and/or forcing, turbulence, thermodynamic systems[12], and systems with feedback, all show chaotic behaviour for certain values of the system inherent parameters.

The Hénon–Heiles model is interesting for two reasons:

(a) it is historically the first example of a model that was shown, via direct computer simulations, to exhibit chaotic behaviour;

(b) it is special for the reason that it is one of a few known examples of a *conservative* system (that is, coming from a potential function) that is chaotic.

It was known since at least from the beginning of the 20th century that there are systems that are very complicated and show unpredictable behaviour (such as the *three-body problem* and Poincaré's proposed solution to this). However, it was not until Hénon and Heiles studied the present model that a thorough study of non-linear phenomena and chaotic behaviour was begun in earnest.

Another interesting feature of the Hénon–Heiles model is that it is conservative. Most chaotic models come from systems that are *dissipative*, i.e., there is a successive loss of energy due to friction or heat transfer, for instance. Dissipative systems are never conservative, so the Hénon–Heiles model belongs to a rather small set of chaotic systems. On the other hand, the fact that the system is conservative means that the equations governing the motion is easy to find and quite simple to solve numerically, as we have seen.

5.3 More information

For more information of the Hénon–Heiles model and non-linear dynamical systems have a look at [Zot15], [LR03] or [HSD04], for instance. There is an infinitude of other papers and books related to the above subject, so if time and other interests are of no importance to you, feel free to scour the web.

References

[HH64] Michel Hénon and Carl Heiles. The applicability of the third integral of motion: Some numerical experiments. *Astronom. J.*, 69:73–79, 1964.

[HSD04] Morris W. Hirsch, Stephen Smale, and Robert L. Devaney. *Differential equations, dynamical systems, and an introduction to chaos*, volume 60

[12] But beware that chaos and entropy, although related, are different phenomena.

of *Pure and Applied Mathematics (Amsterdam)*. Elsevier/Academic Press, Amsterdam, second edition, 2004.

[LR03] M. Lakshmanan and S. Rajasekar. *Nonlinear dynamics*. Advanced Texts in Physics. Springer-Verlag, Berlin, 2003. Integrability, chaos and patterns.

[Zot15] Euaggelos E. Zotos. Classifying orbits in the classical Hénon-Heiles Hamiltonian system. *Nonlinear Dynam.*, 79(3):1665–1677, 2015.